The G protein-coupled receptor regulatory kinase GPRK2 participates in Hedgehog signaling in *Drosophila*

Cristina Molnar*, Helena Holguin*†, Federico Mayor, Jr.*†, Ana Ruiz-Gomez*†‡, and Jose F. de Celis*‡

*Centro de Biología Molecular ''Severo Ochoa'' and †Departamento de Biología Molecular, Universidad Autónoma de Madrid, 28049 Madrid, Spain

Communicated by Antonio Garcia-Bellido, Autonomous University of Madrid, Madrid, Spain, March 16, 2007 (received for review January 23, 2007)

Signaling by Smoothened (Smo) plays fundamental roles during animal development and is deregulated in a variety of human cancers. Smo is a transmembrane protein with a heptahelical topology characteristic of G protein-coupled receptors. Despite such similarity, the mechanisms regulating Smo signaling are not fully understood. We show that Gprk2, a *Drosophila* member of the G protein-coupled receptor kinases, plays a key role in the Smo signal transduction pathway. Lowering *Gprk2* levels in the wing disc reduces the expression of Smo targets and causes a phenotype reminiscent of loss of *Smo* function. We found that Gprk2 function is required for transducing the Smo signal and that when *Gprk2* levels are lowered, Smo still accumulates at the cell membrane, but its activation is reduced. Interestingly, the expression of *Gprk2* in the wing disc is regulated in part by Smo, generating a positive feedback loop that maintains high Smo activity close to the anterior–posterior compartment boundary.

Smoothened | wing disc | imaginal discs

Smo is the key transducer of a conserved signaling pathway regulating many developmental processes in vertebrates and invertebrates (1, 2). The transmembrane protein Patched (Ptc) is the receptor for the ligand Hedgehog (Hh) and represses Smo activity in the absence of ligand (2). The binding of Hh to Ptc relieves this repression and allows Smo to signal to a protein complex that includes the transcription factor Ci/Gli (1). Smo controls the activation of Ci in the presence of the Hh ligand in part by preventing Ci proteolytic processing into a transcriptional repressor. In the *Drosophila* wing disc, the epithelium giving rise to the wing and thorax of the fly, Smo signaling controls the expression of several genes in anterior cells close to the anterior–posterior (A/P) compartment boundary and promotes the growth and patterning of the wing (3–5).

The cytoplasmic tail of *Drosophila* Smo is a target for phosphorylation by protein kinase A and casein kinase I, and it has been shown that Smo phosphorylation by these kinases is essential for its activity and membrane accumulation (6–9). However, most of these phosphorylated residues are not conserved in its vertebrate counterparts (10). Recently, the G protein-coupled receptor kinase 2 (Grk2) has been shown to phosphorylate mammalian Smo (11). G protein-coupled receptor kinases (GRKs) selectively phosphorylate the ligand-activated form of G protein-coupled receptors (12). This phosphorylation promotes uncoupling from G proteins and also the recruitment of β-arrestins, which target the receptor for clathrin-mediated endocytosis. In addition, GRKs and β-arrestins also participate in signal propagation by recruiting additional proteins to the receptor complex (12–14). There are two *Drosophila* GRKs, GPRK1 and GPRK2. GPRK1 modulates the amplitude of the visual response acting as a Rhodopsin kinase, whereas GPRK2 regulates the level of cAMP during *Drosophila* oogenesis (15, 16). Phosphorylation of mammalian Smo by GRK2 promotes its endocytosis in clathrin-coated pits in a process dependent on β-arrestin2 (11). However, whether this form of Smo internalization is part of a desensitization mechanism, as is the case for different G protein-coupled receptors (12), or if it participates in Hh signaling is still not known. To address the participation of GRKs during Smo signaling in *Drosophila*, we have analyzed the function of *Gprk2* during imaginal wing disc development. We found that Gprk2 activity is required for Smo activation. Thus, the reduction of *Gprk2* expression by interference RNA, or its elimination by a genetic mutation, causes the accumulation of Smo in wing disc anterior cells exposed to Hh. The accumulation of Smo is, however, correlated with reduced activity, because Smo high-level targets are not correctly activated and flies expressing *Gprk2-RNAi* display Hh loss-of-function phenotypes. Interestingly, the reduction in *Gprk2* expression is able to antagonize the activity of Smo mutant forms that mimic its phosphorylation by protein kinase A and casein kinase 1, suggesting that additional phosphorylation by Gprk2 is a necessary step to obtain the correct activation of Smo to promote the expression of its targets requiring high levels of signaling.

Results and Discussion

Regulation of *Gprk2* Expression by Hh Signaling in the Wing Disc. The expression of *Gprk2* mRNA in the wing disc is generalized but appears increased in a stripe of cells located close to the A/P compartment boundary (white arrow in Fig. 1*A*). To better characterize this pattern, we used the *P-lacZ* insertion $Gprk2^{06936}$, which is localized in the 5′ untranslated region of the gene (17). Interestingly, β-gal expression is restricted to the A/P compartment boundary of the wing disc during the third larval instar (white arrow in Fig. 1*C*). The cells expressing β-gal were further identified by using a combination of region-specific markers such as Engrailed (En), Patched (Ptc), Blistered (Bs), and Caupolican (Caup) (Fig. 1). This analysis places the stripe of maximal expression of *Gprk2* to anterior cells abutting the A/P boundary. These cells express Ptc and En in the anterior compartment and are localized in the region exposed to high-level Hh signaling. In fact, Hh signaling regulates the expression of *Gprk2* in these anterior cells, because β-gal expression in $Gprk2^{06936}$ discs is expanded to the entire anterior compartment when *hh* is ectopically expressed (Fig. 1*G*), and it is repressed when the activity of the pathway is reduced by ectopic expression of Ptc (Fig. 1 *H* and *I*). The regulation of *Gprk2* accumulation in anterior cells by Hh suggests that Hh signaling and *Gprk2* might be functionally related.

***Gprk2* Is Required for Hh Signaling in the Wing Disc.** All available *Gprk2* alleles are *P* element insertions in the 5′ region of the gene (17). These alleles are homozygous viable, and the mutant wings do

Author contributions: A.R.-G. and J.F.d.C. designed research; C.M., H.H., A.R.-G., and J.F.d.C. performed research; C.M., A.R.-G., and J.F.d.C. analyzed data; and F.M., A.R.-G., and J.F.d.C. wrote the paper.

The authors declare no conflict of interest.

Abbreviations: UAS, upstream activator sequence; GRK, G protein-coupled receptor kinase; A/P, anterior–posterior; FLP, Flipase.

‡To whom correspondence may be addressed. E-mail: aruiz@cbm.uam.es or jfdecelis@cbm.uam.es.

This article contains supporting information online at www.pnas.org/cgi/content/full/0702374104/DC1.

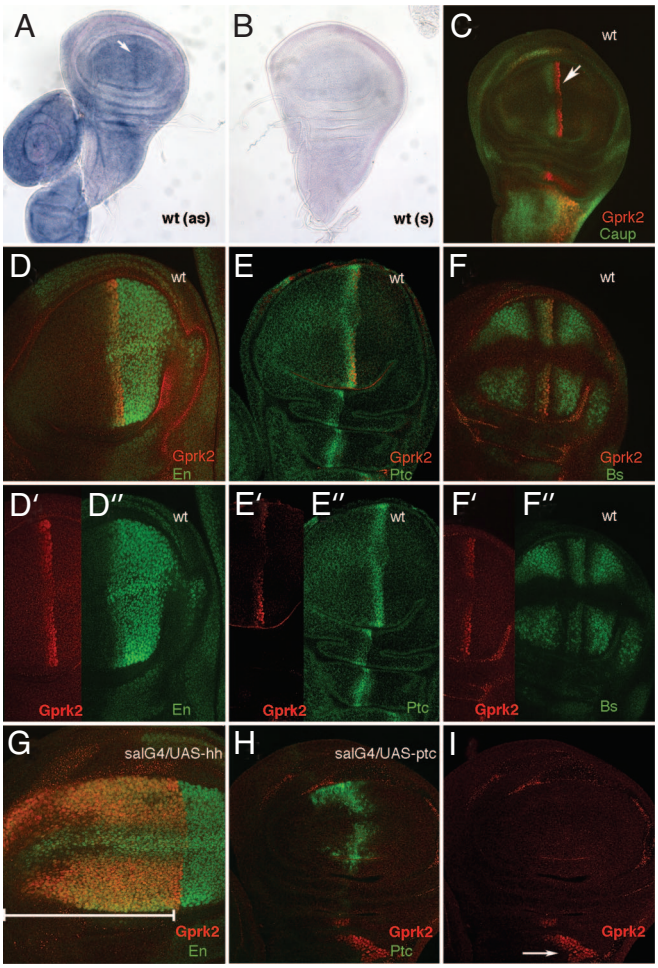

Fig. 1. Enhanced *GPRK2* accumulation in regions of high-level Hh signaling in the wing disc. (*A* and *B*) *In situ* hybridization of third instar wing imaginal discs with *Gprk2* antisense (as) (*A*) and sense (s) (*B*) probes. The expression of *Gprk2* is detected at higher levels in cells abutting the A/P compartment boundary (white arrow in *A*). (*C*) Expression of β-gal (red) and Caupolican (Caup, green) in a third instar wing disc heterozygous for the *P-lacZ* insertion *PZ-Gprk2[06936]*. The white arrow indicates the stripe of β-gal accumulation. (*D*) Expression of β-gal/*Gprk2* (Gprk2, red) and Engrailed (En, green) in wild-type wing disc (wt), showing that β-gal expression occurs in anterior cells expressing En (nuclei in orange). Individual channels are shown in *D′* (Gprk2) and *D″* (En). (*E*) Expression of β-gal/*Gprk2* (Gprk2, red) and Patched (Ptc, green). Individual channels are shown in *E′* (Gprk2) and *E″* (Ptc). (*F*) Expression of β-gal/*Gprk2* (Gprk2, red) and Blistered (Bs, green). Individual channels are shown in *F′* (Gprk2) and *F″* (Bs). (*G*) Expression of β-gal/*Gprk2* (Gprk2, red) and Engrailed (En, green) in *sal-Gal4/+; PZ-Gprk2*$^{[06936]}$*/UAS-hh* wing discs. The extent of β-gal and En expression is included in the bottom white line and appears as orange nuclei. (*H*) Expression of β-gal/*Gprk2* (Gprk2, red) and Patched (Ptc, green) in *sal-Gal4/UAS-ptc; PZ-Gprk2*$^{[06936]}$*/+* wing discs, showing that β-gal expression is eliminated in the wing blade upon ectopic Ptc expression. (*I*) Individual red channel of *H*, showing that the expression of β-gal/*Gprk2* in the thorax (where *sal-Gal4* in not expressed) is not affected (white arrow). wt, wild type.

not display any visible phenotype (data not shown). We generated stronger loss-of-function conditions of the gene by (*i*) expressing *Gprk2* interference RNA (*Gprk2i*) under the control of yeast upstream activator sequences (UAS; *UAS-Gprk2i*) and (*ii*) constructing a synthetic deletion of the gene [see *Materials and Methods* and supporting information (SI) Fig. 6]. In wing discs of the combination *Gal4–638/UAS-Gprk2i*, we found a reduction of *Gprk2* mRNA levels of 66 ± 1.5% (SI Fig. 6*A*). The corresponding adult wings show a range of striking phenotypes similar to loss of Hh function, displaying a reduction of the L3/L4 intervein, fusion of the L3 and L4 veins, and in a lower percentage of wings, the loss of the L3 and L4 veins (Fig. 2 *A–D* and Table 1). These veins and the L3/L4 intervein correspond to the territory specified by Hh signaling (18). In fact, reduction of *Gprk2* levels results in wings very similar to those with a moderate loss of Hh signaling, generated either by ectopic expression of Ptc (Fig. 2*J*) or by expression or *hh*-interference RNA (Fig. 2*G*). This phenotype is very different from that observed upon increased activity of the pathway (see Fig. 5*A*). The *Gal4–638* line is expressed in the entire wing (SI Fig. 6*B*), and to distinguish between the effects of lowering *Gprk2* levels in cells producing or responding to Hh, we used three other Gal4 lines expressed in either the anterior (*Gal4-Ci* and *Gal4-ptc*) or the posterior (*Gal4-hh*) compartments. We found that only the expression of *Gprk2i* in anterior cells recapitulates the reduction of the L3/L4 intervein observed in *Gal4–638/UAS-Gprk2i* wings (Fig. 2 *E* and *F* and data not shown). Thus, the combinations *Gal4-Ci/UAS-Gprk2i* (data not shown) and *Gal4-ptc/UAS-Gprk2i* (Fig. 2*F*) show a reduction or elimination of the L3/L4 intervein, whereas the wings of the *Gal4-hh/UAS-Gprk2i* combination display a normal pattern of veins (Fig. 2*E*). The phenotypes observed upon a reduction of *Gprk2* unambiguously indicate that *Gprk2* function is necessary for the transduction of the Hh signal. Furthermore, when the expression of *Gprk2* is reduced in flies expressing lower levels of the ligand Hh (*Gal4–638/+; UAS-hhi / UAS-Gprk2i*; Fig. 2*H*), the resulting wings have stronger *hh* loss-of-function phenotypes, and a previously unrecognized phenotypic class indistinguishable to those of wings formed by *smo* mutant cells (*Gal4–638/+; FRT42 smo*^{2}*/ FRT42 M (2)l*^{2}*; UAS-FLP/+*; Fig. 2*I*) is now observed (Fig. 2*H* and Table 1).

To directly monitor the activity of the Hh pathway, we studied the expression of several Hh targets in *Gal4–638/UAS-Gprk2i* discs. The expression of En (Fig. 2 *K*, *L*, and *L″* and Table 1) and Ptc (Fig. 2 *M* and *M′* and Table 1) in anterior cells is always impaired when *Gprk2* levels are reduced. These two genes correspond to Hh targets activated by a high level of signaling (18). The expression of Knot (Kn) is also reduced in *Gal4–638/UAS-Gprk2i* discs (Fig. 2 *K′–L′*), and the stripe of maximal accumulation of Ci is also modified in *Gal4–638/UAS-Gprk2i* discs compared with wild-type ones (Fig. 2 *N* and *N′*). We also analyzed in *Gal4–638/UAS-Gprk2i* discs the expression of other genes regulated directly or indirectly by Hh signaling. The expression of the Notch ligand Delta (Dl) is very weak or absent in the primordia of the veins L3 and L4 (Fig. 2*Q′*), where it accumulates at high levels in normal discs (Fig. 2*Q*). Similarly, the expression of Bs in the L3/L4 intervein is reduced or absent in *Gal4–638/UAS-Gprk2i* discs (Fig. 2 *O* and *O′*). The expression of the low-level Hh signaling targets *caup* and *decapentaplegic* (*dpp*) is also modified in *Gal4–638/UAS-Gprk2i* discs. Caup expression in the presumptive L3 vein is generally expanded toward the A/P compartment boundary in *Gal4–638/UAS-Gprk2i* discs (Fig. 2 *R* and *R′*), most likely because En, a repressor of Caup in anterior cells (19), is not expressed upon a reduction of *Gprk2* levels. We found that the domain of Caup expression in the L3 vein is reduced or lost compared with wild-type discs in only a small fraction of discs (7%) (data not shown). The expression of *dpp* is detected in *Gal4–638/UAS-Gprk2i* discs at lower levels but in a domain broader than the characteristic of normal discs (Fig. 2 *S* and *S′*). Taken together, our data suggest that Gprk2 plays a positive role in the Hh signaling pathway. The lowering of *Gprk2* levels reduces very efficiently high-level Hh signaling and much less efficiently low-level Hh signaling. Thus, a complete elimination of Hh signaling is only observed when *Gprk2* levels are reduced in wing discs with lower *hh* (*Gal4–638/+; UAS-hhi / UAS-Gprk2i*; Fig. 2*H*). Finally, the expression of *spalt*, a target of the Dpp/BMP4 pathway (20), is almost normal upon *Gprk2* reduction (Fig. 2 *P* and *P′*), indicating specificity of *Gprk2* function toward Hh signaling.

To confirm the specificity of the *Gprk2 RNAi*, we also analyzed the expression of two Hh-targets, En and Ptc, in wing disc cells

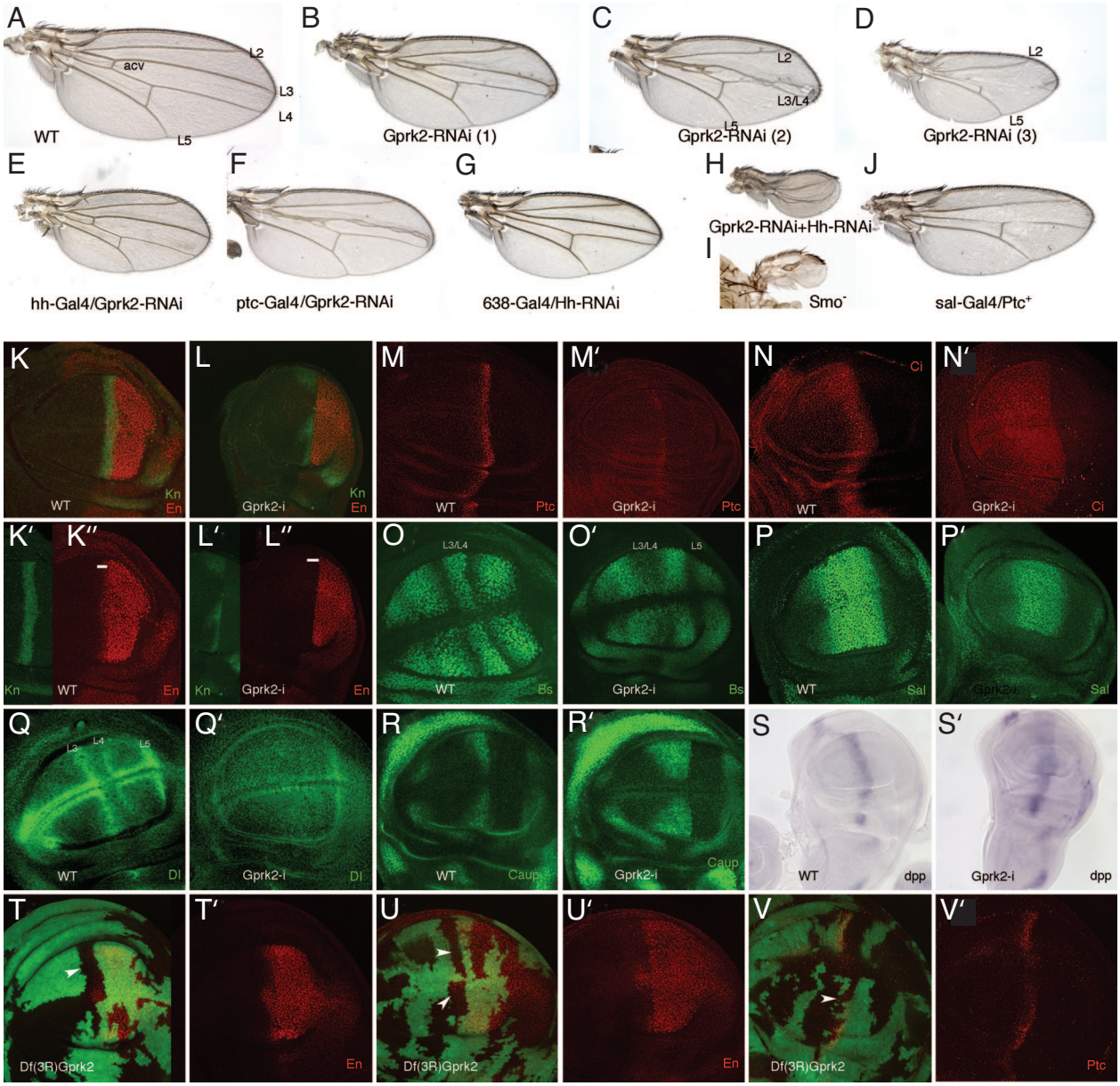

Fig. 2. *Gprk2* is required for Hh signaling. (*A*) Wild-type wing showing the position of the longitudinal veins L2 to L5. acv, anterior cross vein. (*B–D*) Adult wings resulting from ectopic expression of interference *Gprk2* RNA in *Gal4–638/UAS-Gprk2i* flies. Mild phenotypes consist of a moderate reduction of wing size and the shortening of the distance between the L3 and L4 veins [*B*; Gprk2-RNAi (1)]. Medium phenotypes are characterized by partial fusion of the L3 and L4 veins [*C*; Gprk2-RNAi (2)]. Strong phenotypes consist in greater reductions of wing size and the disappearance of the L3 and L4 veins [*D*; Gprk2-RNAi (3)]. (*E*) Adult wing from *Gal4-hh/UAS-Gprk2i* flies, expressing interference *Gprk2* RNA in the posterior compartment. (*F*) Adult wing from *Gal4-ptc/UAS-Gprk2i* flies, expressing interference *Gprk2* RNA in anterior cells close to the A/P compartment boundary (compare to *B* and *C*). (*G*) *Hh* loss-of-function phenotype in *638-Gal4/UAS-hh-RNAi* flies consists of wing size reduction, shortening of the distance between the veins L3 and L4, and loss of the anterior cross vein (acv in *A*). (*H*) Severe *hh* loss-of-function phenotype in *638-Gal4/UAS-hh-RNAi*; *UAS-Gprk2i*/+; compare to the expression of only *hh-RNAi* (*G*) or only *Gprk2-RNAi* (*B–D*). (*I*) Severe *hh* loss-of function phenotype in *Gal4–638/+; FRT42 smo*^{2}*/FRT42 M (2)l*^{2}*; UAS-FLP/+*. These wings, formed by homozygous *smo*^{2} cells, are extremely reduced in size and have lost most pattern elements. (*J*) Hh loss-of-function phenotype caused by ectopic expression of *ptc* (*sal-Gal4/UAS-ptc*) is very similar to loss of *Gprk2* function (compare to *D*). (*K–K″*) Expression of Knot (Kn; *K* and *K′*, green) and Engrailed (En; *K* and *K″*, red) in a third instar wild-type wing imaginal disc. (*L–L″*) Loss of *Gprk2* reduces Knot expression (Kn; *L* and *L′*, green) and eliminates anterior expression of Engrailed (En; *L*, *L″*, red). The white lines in *K″* and *L″* delimit the anterior domain of En expression. (*M* and *M′*) Expression of Ptc in wild-type discs (wt; *M*) and in *Gal4–638/UAS-Gprk2i* (Gprk2-i; *M′*). Loss of *Gprk2* reduces the expression of Ptc. (*N* and *N′*) Expression of Ci in wild-type discs (wt; *N*) and in *Gal4–638/UAS-Gprk2i* wing discs (Gprk2-i; *N′*). (*O* and *O′*) Expression of Bs in wild-type discs (wt; *O*) and in *Gal4–638/UAS-Gprk2i* wing discs (Gprk2-i; *O′*). Loss of *Gprk2* eliminates the L3/L4 intervein domain of Bs expression. (*P* and *P′*) Expression of the Dpp target gene Sal in wild-type (wt; *P*) and *Gal4–638/UAS-Gprk2i* discs (Gprk2-i; *P′*). Overall, the level and anterior-posterior extent of the Sal domain is not affected. (*Q* and *Q′*) Expression of Dl in wild-type discs (wt; *Q*) and in *Gal4–638/UAS-Gprk2i* (Gprk2-i; *Q′*). Loss of *Gprk2* reduces Dl expression in the L3 and L4 veins. (*R* and *R′*) Wing discs showing the expression of Caupolican (Caup) in wild-type (wt; *R*) and *Gal4–638/UAS-Gprk2i* wing discs (Gprk2-i; *R′*). Loss of *Gprk2* expands Caup. (*S* and *S′*) *In situ* hybridization with a *dpp* RNA probe in wild-type (wt; *S*) and *Gal4–638/UAS-Gprk2i* (Gprk2-i; *S′*) wing discs. Upon a reduction in *Gprk2* levels, *dpp* expression occurs at lower levels and in an expanded domain. (*T–V*) Clones of *Df(3R)Gprk2* cells induced in *hs-FLP1.22; FRT82 Df(3R)Gprk2/ FRP82 M (3)w Ubi-GFP* discs at 48–72 h after egg laying. Homozygous *Gprk2*$^{-}$ cells are labeled by the absence of GFP and appear as black spots. In *T* and *T′* and *U* and *U′*, the expression of En (En; red) is shown, and in *V* and *V′*, the expression of Ptc is shown in red. In anterior *Gprk2* mutant cells located close to the A/P compartment boundary, the expression of En (*T–U′*) and Ptc (*V* and *V′*) is not detected. *T′*, *U′*, and *V′* show the red channels of *T*, *U*, and *V*, respectively.

Table 1. Percentage of phenotypic classes observed in genetic combinations involving the overexpression of *Gprk2-RNAi*

	Phenotypic class						En expression			Ptc expression			Smo expression	
Genetic combination	0, %	1, %	2, %	3, %	4, %	No. of wings	Wild type	Reduced	Eliminated	Wild type	Reduced	Eliminated	Wild type	Increased
638/+; Gprk2i/+	29	58	10	3	0	1,145	0	4	10	0	3	11	0	20
638; Gprk2i/+	51	49	0	0	0	37	0	4	6				0	7
638/+; Gprk2i/+; Gprk2i/+	2	29	54	15	0	299								
638/+; Gprk2i/+; Df(3R)Gprk2/+	15	60	16	11	0	123								
638/+; Gprk2i/+; Hhi/+	0	34	32	28	7	224								

Phenotypic classes are represented as 0 (weaker) to 4 (stronger). Data are shown as percentage of wings. En and Ptc columns show the number of wing discs with wild-type, reduced, or eliminated expression of Engrailed (En) and Patched (Ptc) in anterior cells. The Smo column represents the number of wing discs with wild-type or increased expression of Smo in anterior cells. All crosses were done at 29°C with the driver *638-Gal4*.

homozygous for a deficiency that removes all of the *Gprk2* coding region [*Df(3R)Gprk2*; see SI Fig. 6 and *Materials and Methods*]. In both cases we found that anterior *Gprk2*$^-$ clones eliminate, in a cell-autonomous manner, the anterior expression of En (70% of 22 clones; Fig. 2 *T–U′*) and Ptc (Fig. 2 *V* and *V′*). *Gprk2*$^-$ clones located in the posterior compartment did not affect the expression of En, confirming that Gprk2 activity is required in cells receiving Hh.

Gprk2 Participates in the Reception of the Hh Signal. To further analyze where *Gprk2* function is required in the Hh signaling pathway, we studied the expression of En in clones of cells ectopically expressing *hh* or both *hh* and *Gprk2i* (Fig. 3). We found that clones expressing *Gprk2i* located in the domain of En expression in the anterior compartment cell-autonomously suppress the expression of En (Fig. 3 *A–B′*). The expression of En is induced by Hh signaling in *hh*-expressing clones, both within the clone and in the surrounding cells (Fig. 3 *C–C″* and ref. 5). However, in the *hh+Gprk2i*-expressing clones, the expression of En is only induced in wild-type anterior cells that do not express *Gprk2i* (Fig. 3 *D–E″*). These observations confirm that Gprk2 activity is required for transducing the Hh signal in Hh-receiving cells and not for Hh secretion.

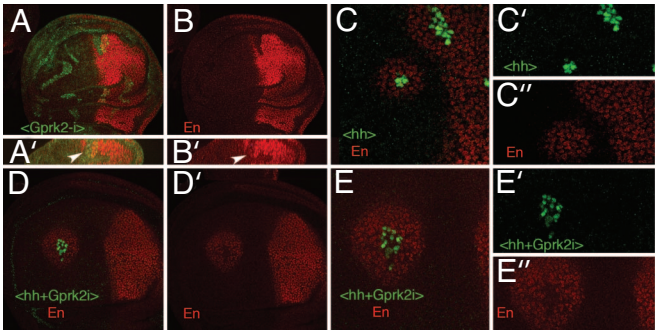

Fig. 3. GPRK2 function is required downstream of Hh. (*A* and *B*) Expression of Engrailed (En, red) in wing discs carrying clones of *Gprki*-expressing cells induced in *hs-FLP; Ubx/abx Gal4-lacZ/UAS-Gprk2i* (*B*) corresponds to the red channel, and the clones are labeled in green. The expression of En is lost in anterior cells. *A′* and *B′* show Z sections of the clones shown in *A* and *B*, respectively. (*C*) Expression of Engrailed (En, red) in wing discs carrying clones of Hh-expressing cells induced in *hs-FLP; Ubx/abx Gal4-lacZ/UAS-hh* larvae (<hh>, green). En is activated in anterior cells both within hh-expressing cells (green) and in the surrounding wild-type cells. Individual channels are shown for En (red, *C″*) and Hh-expressing cells (green, *C′*). (*D–E*) Expression of Engrailed (En, red) in wing discs carrying clones of cells expressing Hh and Gprk2i (<hh+Gprk2i>, green). En is activated in anterior cells surrounding the clones but not within the clone itself. Individual channels are shown below for En (*D′* and *E″*) and (Hh+Gprk2i)-expressing cells (*E′*). *E–E″* are higher magnifications of the clone shown in *C*.

Smo Protein Expression in *Gprk2* Mutant Discs. Experiments in mammalian cells in culture have shown that β-arrestin2 and GRK2 mediate internalization of active Smo (11). Consequently, we studied the expression and subcellular localization of Smo in wing discs where Gprk2 activity is reduced. In wild-type discs, *smo* RNA is expressed in all cells, but Smo protein accumulates associated to cell membranes only in the posterior compartment and in some anterior cells exposed to Hh (7, 9, 21) (Fig. 4*A*). Intriguingly, the reduction in *Gprk2* levels in the entire wing blade eliminates the distinction in Smo accumulation between anterior and posterior cells, and Smo is detected at similar levels in both compartments (Fig. 4 *A* and *B*). When the levels of *Gprk2* are reduced only in the dorsal compartment (*Gal4-ap/UAS-Gprk2i*; Fig. 4*C*) or in clones of *Gprk2*$^-$ homozygous cells (Fig. 4 *D–E*), the changes in Smo expression in anterior cells are more evident. Thus, we observed that Smo accumulates at high levels associated to cell membranes in a broader anterior domain of cells within the range of Hh (Fig. 4 *C–E*). The extension of Smo accumulation in anterior cells might be due to an extension of the Hh diffusion range because Ptc is not expressed in *Gprk2* mutant cells (see ref. 22). This is, to our

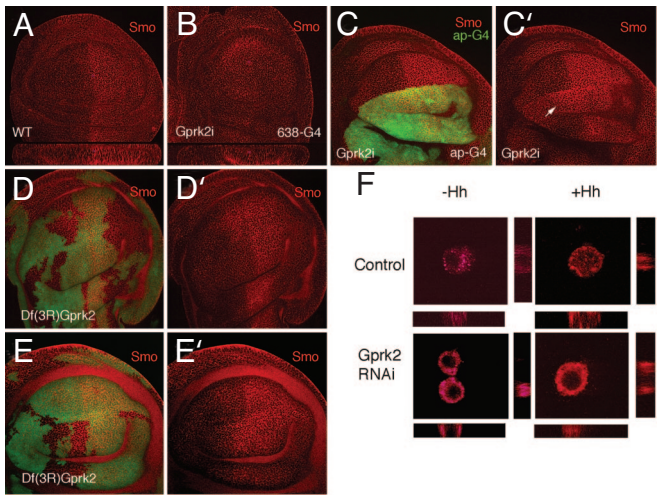

Fig. 4. Smo accumulation depends on Gprk2 activity. (*A* and *B*) Expression of Smo in wild-type (WT; *A*) and *638-Gal4/UAS-Gprk2i* (GPRK2i; *B*) wing discs visualized by using mouse anti-Smo (red). Below each disc is a Z section through the middle of the wing blade. The apical side of the epithelium is up. (*C* and *C′*) Expression of GFP (green) and Smo (red) in *ap-Gal4/UAS-Gprk2i UAS-GFP*. Smo is accumulated in a broader domain in anterior-dorsal cells (white arrow). (*D–E*) Examples of *Df(3R)gprk2* clones (labeled by the absence of green) showing increased expression of Smo (red) in anterior cells located close to the A/P compartment boundary. (*F*) Control S2 cells and S2 cells treated with $dsRNA_{gprk2}$ for 4 days were plated on poly(lysine)-coated slides and incubated for 6 h with S2 or S2HhN-conditioned medium prior to fixation and immunoassayed for Smo.

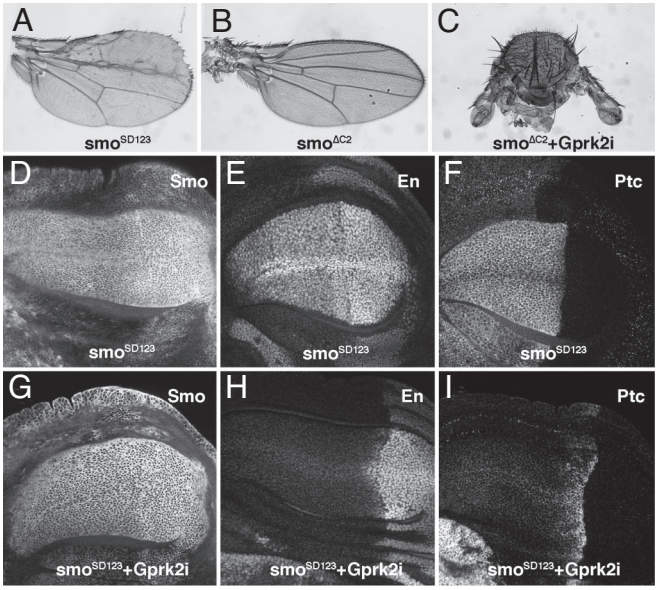

Fig. 5. Interactions between Gprk2 and the intracellular domain of Smo. (*A*) Phenotype caused by the expression of the Smo phosphomimic form SmoSD123 in the wing blade at 25°C. (*B* and *C*) Phenotype caused by ectopic expression of a Smo intracellular deletion (*638-Gal4/UAS-SmoΔC2*; *B*) and severe loss-of-Hh signaling phenotype resulting from the coexpression of *Gprk2* RNAi in this genetic background (*638-Gal4/UAS-SmoΔC2+UAS-Gprk2i*; *C*). (*D–F*) Expression of Smo (*D*), En (*E*), and Ptc (*F*) in wing discs of *638-Gal4/+; UAS-Smo^{SD123}/+* genotype. Note the expansion of Smo, En, and Ptc domains of expression to the entire anterior compartment. (*G–I*) Expression of Smo (*G*), En (*H*), and Ptc (*I*) in wing discs of *638-Gal4/+; UAS-Smo^{SD123} /UAS-Gprk2i* genotype. The anterior expression of En (*H*) and Ptc (*I*) is now suppressed upon a reduction in *Gprk2* levels. Despite of the presence of the Smo^{SD123} protein in the cell membrane of anterior cells (*G*), the pathway does not activate the expression of the high-level targets En and Ptc.

knowledge, a previously unrecognized instance in which Smo accumulation and signaling can be uncoupled, because it was thought that, at least in *Drosophila*, Smo membrane accumulation leads to signaling. The same effects are observed when S2 cells were used (Fig. 4*F*). Thus, Smo is expressed in S2 cells in intracellular vesicles at low levels (Fig. 4*F Upper Left*). Upon Hh treatment, Smo translocates close to the plasma membrane in these cells (Fig. 4*F Upper Right*). In cells that have been treated for 4 days with *Gprk2* dsRNA (causing a reduction of *Gprk2* mRNA levels of 77 ± 1.5%; data not shown) the levels of Smo are higher independently of Hh (Fig. 4*F Lower*).

To further analyze the relationship between Smo and Gprk2 functions, we expressed, in the same wing, *Gprk2i* with different N-terminal (smoΔN; extracellular) and C-terminal (smoΔC2 and smoΔC4; intracellular) deletions of Smo (9). The expression of Smo proteins bearing either N-terminal or C-terminal deletions fails to rescue Smo mutants (9), but their overexpression does not interfere significantly with Smo signaling (*638-Gal4/UAS-smoΔC2*; Fig. 5*B* and data not shown). We found a strong synergic genetic interaction when Smo C-terminal deletions (ΔC2; AT724 and ΔC4; AS939) (9) were coexpressed with *Gprk2i* (*638-Gal4/UAS-smoΔC2+UAS-Gprk2i*; Fig. 5*C* and data not shown). Thus, wings expressing C-terminal deletions of Smo with reduced *Gprk2* levels display a strong *hh* loss-of-function phenotype that is comparable to the elimination of *smo* (see Fig. 2*I*). *Gprk2i* combined with UAS-smoΔN resulted in additive phenotypes (data not shown). We suggest that the reduction of *Gprk2* uncovers a dominant-negative effect of SmoΔC proteins, reducing the efficiency of Smo signaling. The basis for this dominant negative effect could be the inclusion of a form of Smo, SmoΔC, unable to be phosphorylated by Gprk2, in the Smo complexes that have been postulated to mediate Smo activity (23). Therefore, we propose that Gprk2 function, acting through the C-terminal tail of Smo, is involved in an activation step promoting Smo interaction with the Costal2/Fused/Su(fu) complex to prevent Ci processing into a repressor form and to accumulate Ci in an activating form. Based on the effects of mammalian GRK2 and β2-arrestin on Smo (11, 24), it is possible that Gprk2-mediated activation of Smo involves the recycling of Smo from the cell membrane to an intracellular signaling compartment.

The interaction between SmoΔC and *Gprk2* indicates a critical role of the Smo intracellular C-terminal domain for its relationship with Gprk2 function. Interestingly, the Smo intracellular C-terminal domain is where all of the consensus phosphorylation sites by casein kinase 1 and protein kinase A are located, as well as other serine and threonine residues in the vicinity of acidic residues that are similar to mammalian GRK2 phosphorylation consensus (25, 26). We expressed in the wing disc a form of Smo that mimics its phosphorylation by these kinases (Smo^{SD123}; ref. 8) and analyzed whether this Smo-activated form is sensitive to Gprk2 levels. The expression of Smo^{SD123} in the wing disc causes overgrowth of the anterior compartment and defects in the L3 and L2 veins (Fig. 5*A*). In the corresponding wing discs, the accumulation of Smo and the expression of its targets En and Ptc are expanded to occupy the entire anterior compartment (Fig. 5 *D–F*). When *Gprk2* levels are reduced in discs expressing Smo^{SD123}, Smo accumulation is still observed in all anterior cells (Fig. 5, compare *G* with *D*). In contrast, the expression of both En and Ptc is now restricted to their normal domains adjacent to the A/P compartment boundary (Fig. 5, compare *H* and *I* with *E* and *F*). The overgrowth phenotype characteristic of *Gal4–638/+; UAS- Smo^{SD123}* discs (Fig. 5 *D–F*) is not rescued by the reduction of *Gprk2* expression (Fig. 5 *G–I*), suggesting that the low-level Hh target *dpp* is still expressed through the anterior compartment. These data suggest that to generate the high levels of Smo activity required to activate the expression of its targets En and Ptc, the Smo^{SD123} protein has to be phosphorylated by Gprk2.

Conclusions

Drosophila Gprk2 is critically required to generate high levels of Hh signaling in the wing disc. The genetic interactions between Gprk2 and Smo proteins bearing C-terminal deletions or Smo phosphomimic variants suggest that Smo is a target of Gprk2. The modifications in Smo protein accumulation detected in wing discs and S2 cells with reduced *Gprk2* expression suggests that a likely step affected by Gprk2 is the activation of Smo by a phosphorylation step that could prime Smo for internalization to a signaling compartment. GRK2 has recently been shown to play a positive role in Shh transduction in mammalian cells (24). Taken together, these findings and our data indicate that Smo phosphorylation by GRK homologues constitute a conserved component of the Smo signal transduction cascade.

Materials and Methods

Genetic Strains. We used the *Gprk2* alleles *Gprk2^{EY09213}*, *Gprk2^{06936}*, and *Gprk2^{PL00297}*, the *Smo^{2}* null mutation, the Gal4 lines *Gal4–638*, *Gal4-ptc*, *Gal4-hh*, *Gal4-Ci*, and *Gal4-sal*, and the UAS lines *UAS-hh*, *UAS-ptc*, *UAS-Smo^{SD123}*, *UAS-FLP*, *UAS-GFP*, *UAS-smoΔC2*, *UAS-smoΔC4*, and *UAS-smoΔN* (8, 9). UAS-hhi flies were provided by the National Institute of Genetics (Mishima, Japan) stock center. The expression of *Gal4–638* is restricted to the wing pouch since the second larval instar (see SI Fig. 6). Lines not described in the text can be found in FlyBase (17). Unless otherwise stated, crosses were done at 29°C.

Generation of *UAS-Gprk2i*. The EST LD42147 was used as template for amplification of a 500-bp Gprk2 C-terminal fragment. The amplified fragment was cloned into pSTBlue-1 (Novagen, Madison, WI), from which the fragments BamHI+SacI and SphI+NotI were

DEVELOPMENTAL BIOLOGY

purified. The BamHI-SacI fragment was cloned in pHIBS and digested with SphI and XhoI. The fragments SphI-NotI and SphI-XhoI were cloned in pBluescript II SK+ (Stratagene, La Jolla, CA). The insert was liberated with KpnI and NotI and cloned in pUAST (27). Several UAS-Gprk2i were established after germ-line transformation following standard procedures.

Generation of a *Gprk2* Deficiency. We used the Exelixis flanking insertions *f00526* and *d09952* (28) separated by 54 kb including *Gprk2* and the 5′ untranslated end of CG11337. Flipase (FLP)-induced recombination target recombination was induced by a daily 1-h heat shock at 37°C to the progeny of *hsFLP1.22/+; f00526/d09952* females and *w; TM2/TM6b* males. Eight putative *w; f00526-d09952/TM2* offspring males of *white* phenotype were individually crossed to *w; TM2/TM6b* females and after 3 days were used to extract genomic DNA to confirm by PCR the existence of FLP recombination target recombination. The position of the Exelixis flanking insertions *f00526* and *d09952* and the extent of the *Gprk2* deficiency are described in SI Fig. 6.

Generation of FLP–FLP Recombination Target Clones. We induced clones of cells expressing *hh* or *Gprk2i* and *hh* by a 10-min heat shock in larvae of *hsFLP; abx/Ubx<f+>lacZ-Gal4/UAS-hh* and *hsFLP; abx/Ubx<f+>lacZ-Gal4/UAS-hh UAS-Gprk2i*, respectively. The elimination of the f^+ cassette by FLP-mediated recombination allows the expression of a dicistronic *lacZ-Gal4* gene (29). Clones were identified by the expression of β-gal. Wings homozygous for smo^2 were generated in *Gal4–638/+; FRT42 smo^2/FRT42 M (2)l^2; UAS-FLP/+*. Homozygous *Df(3R)Gprk2* M^+ clones were induced in larvae of genotype *hsFLP1.22; FRT82 Df(3R)Gprk2 / FRT82 M (3)w Ubi-GFP*. Homozygous *Df(3R)Gprk2* cells were recognized in the wing disc by the absence of the GFP marker.

Cell Culture. S2 cells were cultured in the Schneider's *Drosophila* serum-free medium (Invitrogen, Carlsbad, CA) with 10% FCS, 100 units/ml penicillin, and 100 μg/ml streptomycin. Transfection was carried out by using the Cellfectin Reagent Kit (Invitrogen) following the manufacturer's instructions. HhN inducible vector was provided by Stephen M. Cohen (European Molecular Biology Laboratory, Heidelberg, Germany). Stable cell lines overexpressing HhN were generated by puromycin treatment, and Hh S2-conditioned medium was obtained by incubation with 0.7 mM $CuSO_4$ for 24 h as described (21). To reduce *Gprk2* levels using an RNAi approach in S2 cells, we incubated them with 30 μg/ml of *Gprk2* dsRNA (see below) in serum-free medium for 1 h followed by addition of 10% FCS and incubated for an additional 3–4 days to allow protein turnover before treatment with control or Hh-conditioned medium for an additional 6 h. The cells were plated and assayed for *Gprk2* RNA quantification and processed for immunofluorescence.

Double-Stranded *Gprk2* RNA Preparation. We used the *Gprk2* EST as template for amplification of Gprk2 DNA template flanked by T7 RNA polymerase binding sites. dsRNA was generated by *in vitro* transcription by using the Ambion MEGAsript T7 kit (Ambion, Austin, TX).

RNA Isolation and Quantitative Real-Time RT-PCR. Total RNA was prepared from a pool of 30 wing discs (both wild type and Gal4–638/UAS-GPRk2i) or S2 cells by using the TRIzol reagent RNA protocol following Life Technologies (Grand Island, NY) instructions. Total RNA (0.7 μg) was used for a first round of reverse transcription by using the Gene Amp RNA PCR kit (Applied Biosystems, Foster City, CA). Quantitative PCR analysis was performed in a ABIPRISM 7.000 (Applied Biosystems) by using the *Taq*Man probe from Applied Hs99999901_s1 for 18S rRNA and the *Taq*Man UP probe no. 61 from Universal Probe Library (Roche, Indianapolis, IN) for *Gprk2* and 20 ng of the corresponding cDNA. Quantification of mRNA reduction was performed with the ΔΔCt method.

Immunocytochemistry. We used rabbit anti-Kn (18), anti-Sal (30), antiactivated Cas3 (Cell Signaling, Beverly, MA), mouse monoclonal anti-Bs (31), rat anti-Caup (32), and anti-Ci (33). From the University of Iowa Developmental Studies Hybridoma Bank (Iowa City, IA), we used the mouse monoclonals anti-En, anti-Ptc, and anti-Smo. Secondary antibodies were from Jackson ImmunoResearch (West Grove, PA) (used at 1:200 dilution). Imaginal wing discs were dissected, fixed, and stained as described in ref. 34. Confocal images were captured by using a confocal microscope (Bio-Rad, Hercules, CA). *In situ* hybridization with *dpp* and *Gprk2* RNA probes was carried out as described in ref. 34. We used the EST *LD42147* as a template to synthesize the *Gprk2* probe.

We thank A. López-Varea and R. Hernández for their skillful technical help and P. Ingham (Centre for Developmental and Biomedical Genetics, University of Sheffield, Sheffield, U.K.), S. Cohen, and the National Institute of Genetics for providing tools necessary for this work. This work was supported by Dirección General de Investigación Científica y Técnica Grants BCM2003-1191 and GEN2001-4846-C05-01 (to J.F.d.C.) and SAF2005-03053 (to F.M.) and an institutional grant from Fundación Ramón Areces to the Centro de Biología Molecular "Severo Ochoa."

1. Lum L, Beachy PA (2004) *Science* 304:1755–1759.
2. Hooper JE, Scott MP (2005) *Nat Rev* 6:306–317.
3. Tabata T, Kornberg TB (1994) *Cell* 76:89–102.
4. Zecca M, Basler K, Struhl G (1995) *Development (Cambridge, UK)* 121:2265–2278.
5. Strigini M, Cohen SM (1997) *Development (Cambridge, UK)* 124:4697–4705.
6. Zhang C, Williams EH, Guo Y, Lum L, Beachy PA (2004) *Proc Natl Acad Sci USA* 101:17900–17907.
7. Zhu AJ, Zheng L, Suyama K, Scott MP (2003) *Genes Dev* 17:1240–1252.
8. Jia J, Tong C, Wang B, Luo L, Jiang J (2004) *Nature* 432:1045–1050.
9. Nakano Y, Nystedt S, Shivdasani AA, Strutt H, Thomas C, Ingham PW (2004) *Mech Dev* 121:507–518.
10. Huangfu D, Anderson KV (2005) *Development (Cambridge, UK)* 133:3–14.
11. Chen W, Ren XR, Nelson CD, Barak LS, Chen JK, Beachy PA, de Sauvage F, Lefkowitz RJ (2004) *Science* 306:2257–2260.
12. Lefkowitz RJ, Shenoy SK (2005) *Science* 308:512–517.
13. Kohout TA, Lefkowitz RJ (2003) *Mol Pharmacol* 63:9–18.
14. Penela P, Ribas C, Mayor F, Jr (2003) *Cell Signal* 15:973–981.
15. Schneider LE, Spradling AC (1997) *Development (Cambridge, UK)* 124:2591–2602.
16. Lannutti BJ, Schneider LE (2001) *Dev Biol* 233:174–185.
17. The FlyBase Consortium (2005) *Nucleic Acids Res* 33:390–395.
18. Crozatier M, Glise B, Vincent A (2002) *Development (Cambridge, UK)* 129:4261–4269.
19. Gomez-Skarmeta JL, Modolell J (1996) *Genes Dev* 10:2935–2945.
20. Barrio R, de Celis JF (2004) *Proc Natl Acad Sci USA* 101:6021–6026.
21. Denef N, Neubuser D, Perez L, Cohen SM (2000) *Cell* 102:521–531.
22. Chen Y, Struhl G (1996) *Cell* 87:553–563.
23. Hooper JE (2003) *Development (Cambridge, UK)* 130:3951–3963.
24. Reya RJ, Lefkowitz RJ, Caron MG (2006) *Mol Cell Biol* 26:7550–7560.
25. Yoshida N, Haga K, Haga T (2003) *Eur J Biochem* 270:1154–1163.
26. Deupree JD, Borgeson CD, Bylund DB (2002) *BMC Pharmacol* 2:9.
27. Brand AH, Perrimon N (1993) *Development (Cambridge, UK)* 118:401–415.
28. Parks AL, Cook KR, Belvin M, Dompe NA, Fawcett R, Huppert K, Tan LR, Winter CG, Bogart KP, *et al.* (2004) *Nat Genet* 3:288–292.
29. de Celis JF, Bray S (1997) *Development (Cambridge, UK)* 124:3241–3251.
30. de Celis JF, Barrio R, Kafatos FC (1999) *Development (Cambridge, UK)* 126:2653–2662.
31. Nussbaumer U, Halder G, Groppe J, Affolter M, Montagne J (2000) *Mech Dev* 96:27–36.
32. Gómez-Skarmeta JL, Díez del Corral R, de la Calle E, Ferrer-Marcó D, Modolell J (1996) *Cell* 85:95–105.
33. Aza-Blanc P, Ramirez-Weber FA, Laget MP, Schwartz C, Kornberg TB (1997) *Cell* 89:1043–1053.
34. de Celis JF (1997) *Development (Cambridge, UK)* 124:1007–1018.